NJC

Accepted Manuscript

This is an *Accepted Manuscript*, which has been through the Royal Society of Chemistry peer review process and has been accepted for publication.

Accepted Manuscripts are published online shortly after acceptance, before technical editing, formatting and proof reading. Using this free service, authors can make their results available to the community, in citable form, before we publish the edited article. We will replace this *Accepted Manuscript* with the edited and formatted *Advance Article* as soon as it is available.

You can find more information about *Accepted Manuscripts* in the Information for Authors.

Please note that technical editing may introduce minor changes to the text and/or graphics, which may alter content. The journal's standard Terms & Conditions and the Ethical guidelines still apply. In no event shall the Royal Society of Chemistry be held responsible for any errors or omissions in this *Accepted Manuscript* or any consequences arising from the use of any information it contains.

ROYAL SOCIETY OF CHEMISTRY

www.rsc.org/njc

Journal Name

RSCPublishing

ARTICLE

Synthesis Au-ZnO hybrid nanostructure arrays and its enhanced photocatalytic activity

Cite this: DOI: 10.1039/xoxxoooooox

Sun Yuyang, Jiang Long, Zeng Tian, Wei Jing, Liu Ling, Jing Yong, Jiao Zhifeng, Sun Xiaosong*

Received ooth January 2012,
Accepted ooth January 2012

DOI: 10.1039/xoxxoooooox

www.rsc.org/

Abstract: The preparation of Au-ZnO hybrid nanostructructure array on the TCO substrate has been achieved via annealing Au coated ZnO nanorods array in nitrogen atmosphere. The characterizations on the morphology and the structure of Au-ZnO hybrid nanostructructure were carried out with X ray diffraction, scanning electron microscopy and transmission electron microscopy. Photoluminescence spectra give the quenched luminescent emission because of the charges separation in the prepared Au-ZnO hybrid nanostructructure. It is worth pointing out that the prepared Au-ZnO hybrid nanostructructure present much superior photocatalytic activity over ZnO nanorods in case of degradation procedure of methyl orange. It is found that 8 ml methyl orange aqueous solution (2.5 ppm) could be totally degradated with 4 sheets of Au-ZnO hybrid nanostructructure (12×12 mm^2) within 4 hours.

Introduction

Combining disparate nanoscaled components into the hybrid nanostructure (HNs) has been an important research domain for the synthesis and application of nanomaterials. Nowadays, HNs can be formed by interfacing two nanostructures of semiconductors, a metal and a semiconductor or two metals and so on. Multi-component HNs can not only harvest the multi functionalities contributed from each component but also may present enhanced or even new functionalities due to synergetic effects between different components. For example, the properties of biocompatible and suitable for linking different functional molecules were found in Au-Fe_3O_4 HNs [1]; enhanced catalytic properties have also been demonstrated in Ag-Ni core–shell nanoparticles [2] (NPs), CdS-PdX (X: S, O) HNs [3] or Bi_2S_3-$Bi_2O_2CO_3$ [4]. HNs, by far, have been found potential applications in many fields, including biological tagging, medical diagnostics and treatment, solar energy conversion, lithium batteries, gas sensing, and photocatalysis.[4-17]

Recently, HNs, such as CdS/Me18, CdSe/Me and CdS/CdSe/Me19, have been intensively investigated. Thus, significant progresses have been made. For example, Lian et al18 expounded the mechanism of exciton quench and charge transfer in the CdS/Pt hetero metal semiconductor nanostructure by means of ultrafast transient absorption spectroscopy. They proved that the excitons in the CdS domain would dissociate by ultrafast transfering electrons from CdS to Pt and the separated state would surprisingly survive for a long time due to the trapping of holes in CdS or electrons in Pt nanoparticles (NPs). Wu et al[19] prepared CdSe/CdS dot-in-rod nanorods (NRs) with a Pt tip at one end. According to the effect of trapping electrons in the metal tip, they considered this kind of HNs was the promising material for solar-to-fuel conversion because of the rational integration of a light absorber, hole acceptor, and electron acceptor.

Recently, one of the most interesting studied metal-semiconductor hybrids would like to be the metal-ZnO HNs. It is well known that ZnO is an environmentally friendly semiconductor with a direct band gap of 3.37 eV and an exciton binding energy of 60 mV, respectively. Extensive researches focusing on preparations and applications, particularly in photocatalysis of nanoscaled ZnO materials, have been conducted in the materials science and technology community.[20-22] Being a direct band gap material, significant photoelectrons might be excited from valance band (V-band) to conduction band (C-band) with proper ultraviolet (UV) light, leaving holes in the V-band in the meantime, these photo-electrons and holes are the protagonist in the photocatalytic process. However, the quick recombination of the photo-excited electrons and holes in ZnO always leads to reduced photocatalytic efficiency. Therefore, in order to achieve high efficient photocatalytic process, it is vital to suppress the combination of photo-induced electrons and holes by means of separating photo-induced charges. Noble metal NPs such as Au[23, 24], Ag[25, 26] and Pt[27, 28] have been used to form HNs with ZnO to achieve charge transfer and, thus, to enhance photocatalytic activities. Several approaches have been reported to prepare Au-ZnO HNs to meet the inquiry of its photocatalytic. For example, both Li et al[24] and Yao et al[29] have prepared ZnO nanopyramids attached with Au NPs by means of wet chemical process to study their optical property and photocatalytic performance. Pacholski et al [30] have demonstrated site specific photodeposition of single silver NPs on ZnO NRs; in which UV light was used to form well-defined silver NPs.

The past few years have been witness to the progress of HNs synthesis from dual components into complex systems. However, it is even still a great challenge to achieve large-scale, high-yield synthesis of HNs with efficient photocatalytic performance by simple and low-cost approaches. In the present article, we report the simple approach of synthesis and characterization of Au-ZnO HNs. Unlike other published papers in which the preparations of noble metal NPs and semiconductor nanostructures would be carried out independently, a direct and easily scaled method of synthesizing of Au-ZnO HNs array have been employed in this study. The as-

prepared Au-ZnO HNs is of large area, perfect structure between Au NPs and ZnO NRs. Most interesting, the as-prepared Au-ZnO HNs has presented excellent performance in photocatalysis.

Experimental

All the chemicals were analytical grade reagents and used as received without further purification. ZnO NRs were grown on TCO glass substrate using electrochemical deposition in the aqueous solution of $Zn(NO_3)_2 \cdot 6H_2O$ (0.01 M) for 30 min at 80 ^oC. The detail experimental procedure may be found in our previous paper, [31] while the applied potential in the present study was -1V vs SCE, a bit different from that used in Ref. 31. After electrochemical deposition process, Au thin film was deposited on the prepared ZnO NRs using magnetron sputtering for 30 s. The controlled experiments were carried out for evaluating the effect of the amount of Au used. Au coated ZnO NRs were, then, annealed at 200 ^oC for 2 h in nitrogen atmosphere to form the Au-ZnO HNs.

The characterizations on the crystalline structure of the ZnO NRs were performed by X-ray diffraction (XRD, DX1000, Cu Kα radiation) and the morphology and EDX detection of the ZnO NRs were performed by field emission scanning electron microscope (FE-SEM, S4800, Hitachi) and the attached EDX equipment, respectively. The photoluminescence spectra of ZnO NRs or An-ZnO HNs were measured at room temperature with a fluorescence spectrophotometer (F-7000, Hitachi, Xe lamp). The fine crystal structure of the ZnO and that of An-ZnO HNs were analyzed with high resolution transmission electron microscope (HR-TEM, FEI, Tecnai G2 F20 S-TWIN). In order to characterize the photocatalytic performance of An-ZnO HRs, photodegradation of MO was performed at room temperature under UV lamp (365 nm) with four pieces of prepared An-ZnO sheets (12×12 mm^2). The initial concentration of MO solution was fixed at 2.5 ppm. Due to its strong absorption at 465 nm, the measurement of the absorbance at 465 nm vs the concentration of the MO solution was carried out to evaluate the degradation effeciency of MO. The optical absorption spectra were measured with a UV–vis spectrophotometer (UNICO UV2102PC) with a deuterium discharge tube and a tungsten iodine lamp.

Results and discussion

In this study, after annealed at the specific temperature, Au film had become Au NPs and formed the HNs with ZnO NRs array. The characterizations on the structure and performance of Au-ZnO HNs as an efficient and feasible material in photocatalysis had been carried out in detail.

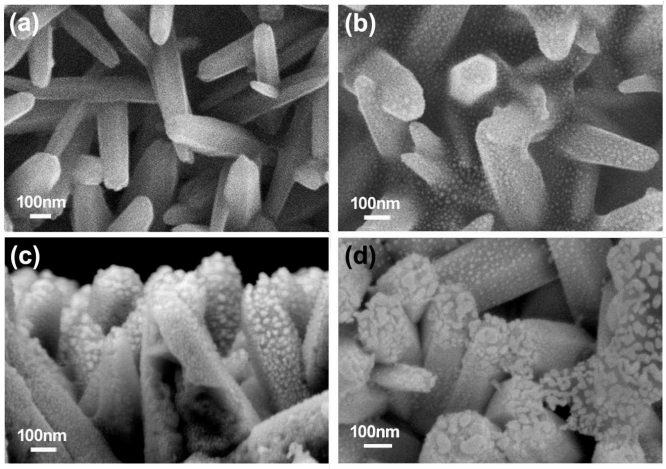

Figure. 1 FE-SEM images of (a) electrochemical deposited ZnO NRs array; (b) top or (c) cross-sectional images of Au-ZnO HNs, respectively, and (d) FE-SEM image of Au-ZnO HNs after 4h photocatalysis.

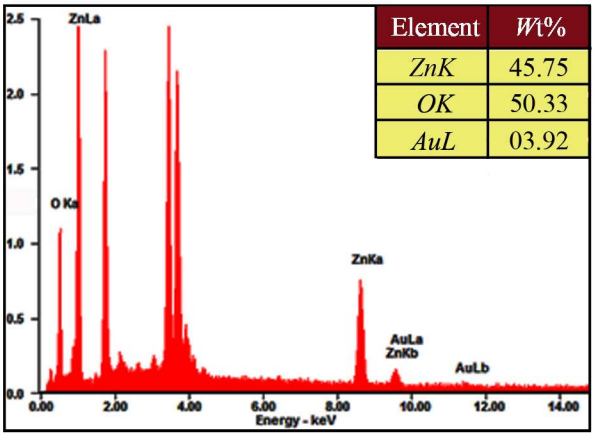

Figure.2 The EDX spectrum of Au-ZnO HNs.

The morphologies of ZnO NRs or Au-ZnO HNs grown on TCO glass substrate are shown in Figure. 1. Figure. 1a is the top view of ZnO NRs array; Figure. 1b and 1c are the top or side views, respectively, of Au-ZnO HNs arrays. From the pictures shown in Figure. 1, it can be clearly seen that the diameter and the length of ZnO NRs was about 150 nm and 500 nm, respectively, and, from Figure 1c, particularly, it can be found that Au thin film had shrinked into Au NPs of 10-20 nm in diameter. Seeing Figure 1d, the morphology of Au-ZnO HNs had little change after 4h photocatalysis. Figure 2 is the EDX analysis of the sample (the peaks, having not been marked, referred to the elements of Sn and Si from substrate, respectively), with which Au was clearly detected and the amount of Au was relatively small.

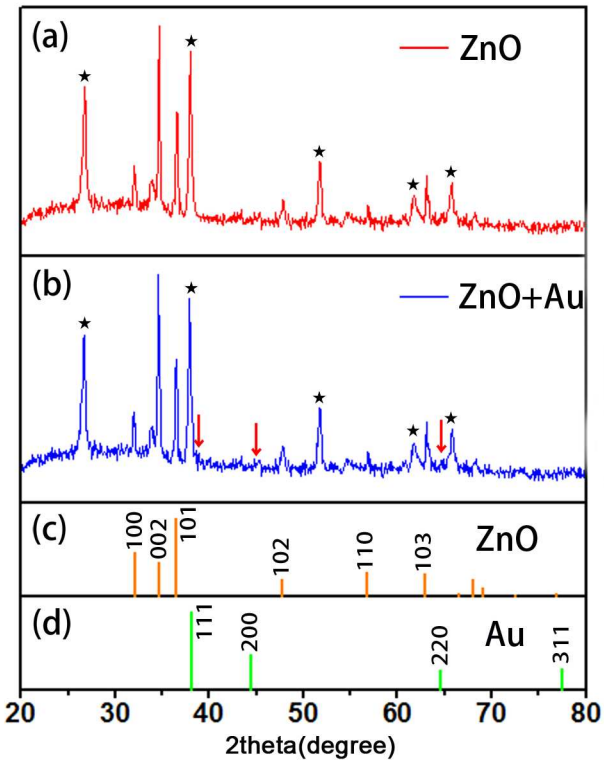

Figure. 3 XRD patterns of ZnO NRs (curve a) and Au-ZnO HNs (curve b) (the peaks marked with asterisk belongs to TCO). The XRD patterns for Au is marked with arrows.

The XRD patterns of ZnO NRs and Au-ZnO HNs are shown in Figure. 3. Apart from the reflections corresponding to the TCO glass substrate, marked with asterisk, the diffraction peaks can be indexed to the wurtzite ZnO (JCPDS 36-1451). From Figure. 3, one could deduce that ZnO NRs might grow in [0002] direction. Because of the Au-ZnO HNs contained a bit of gold, the XRD patterns of which were very weak and particularly marked with arrows. SAED patterns proved the HNs of Au-ZnO NRs, Figure 4d.

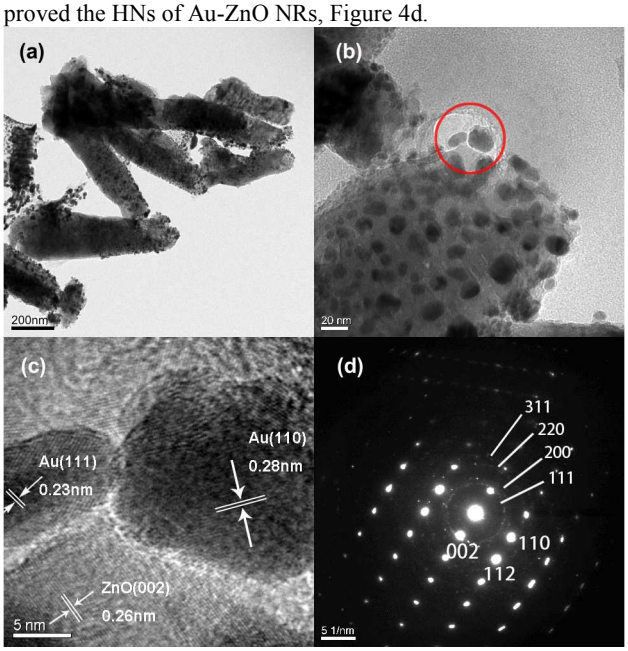

Figure. 4 TEM images of Au-ZnO HNs: (a) low magnification and (b) high magnification, (c) HR-TEM image of Au-ZnO HNs, and (d) SAED patterns of Au-ZnO HNs.

In order to characterize the fine structures of Au-ZnO HNs in detail, the as-prepared Au-ZnO HNs was scraped down from TCO glass substrate, dispersed in ethanol via ultrasonic bath, and then, the ethanol solution was dropped on the copper grid for TEM characterization. Figure. 4 shows the TEM images of the as-prepared Au-ZnO HNs, Figure. 4a-4c, and selective area electron diffraction pattern (SEAD), Figure. 4d. In Figure. 4a and 4b, one could find that there were lots of Au NPs of 10-20 nm in diameter on the surface of ZnO NRs. Figure. 4c is the HR-TEM image of the circled area in Figure. 4b, from which it is certain that the ZnO NRs in Au-ZnO HNs was of single-crystalline structure of [0002] growth direction. The fringes spacing taken from the Au NPs was 0.28 nm for Au {110} and 0.23 nm for Au {111}, respectively. From Figure.4c, it could be found that Au NPs and ZnO NRs were connected with a buffer. The typical SAED patterns of Au-ZnO HNs can be easily discerned and indexed. For example, in Figure. 4d, the brightness dots in the matrix can be attributed to the (002), (110) and (112) planes of ZnO, whereas, a set of unconspicuous diffraction rings can be indexed as (111), (200), and (220) for Au, respectively.

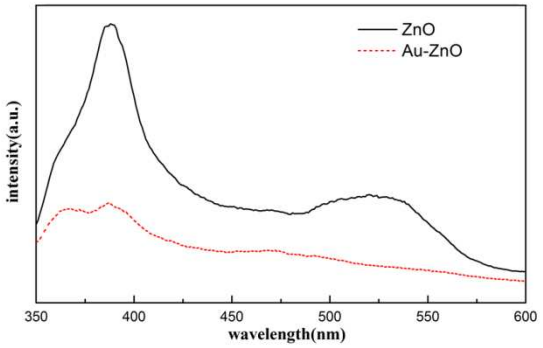

Figure. 5 PL spectra of ZnO NRs (solid line) and Au-ZnO HNs (dashed line) with the excitation of 325 nm at room temperature

Figure. 5 shows the PL spectrum of the Au-ZnO HNs and that of ZnO NRs, respectively, with the excitation of 325 nm at room temperature. The PL spectrum of ZnO NRs (solid line) possesses the feature of two emission bands in UV-visible range, i.e. one is the near-band-edge (NBE) emission centered at 385 nm and the other one is a broadening green emission centered at 525 nm. According to the related researches, the NBE emission could be attributed to the free excitons transition between C-band and V-band,[20] while the green emission was ascribed to the recombination the photo-generated holes and the electrons occupied in oxygen vacancies. [30] It is worth noting that, comparing with two PL spectra, the intensity of the spectrum of Au-ZnO HNs (dashed line) was much weaker than that of ZnO NRs (solid line) because of charge transfer in Au-ZnO HNs[33], which matches well with the previous reports.

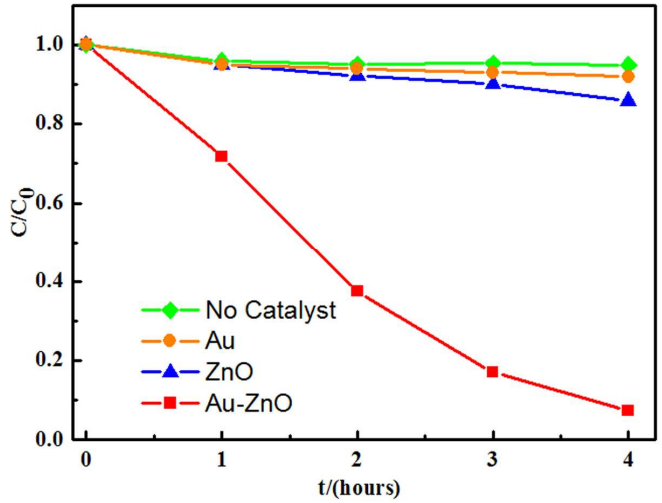

Figure. 6 Photocatalytic performance of ZnO NRs, Au particles and Au-ZnO HNs in MO aqueous solution under UV light (365 nm) at room temperature.

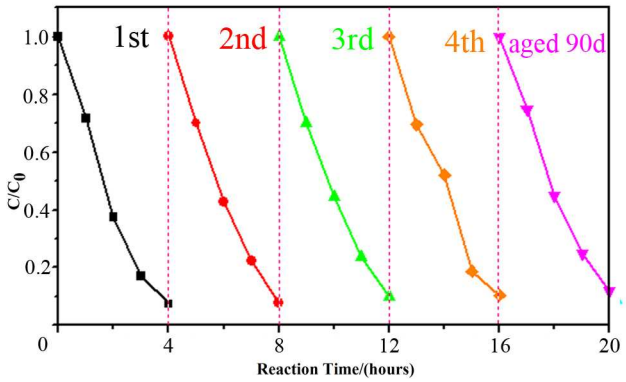

Figure. 7 Cycling photocatalytic reduction of MO over Au-ZnO HNs under UV light (365 nm) at room temperature.

In order to test the photocatalytic activity of as-prepared Au-ZnO HNs, the photodegradation of dye methyl orange (MO) have been conducted out with ZnO NRs, Au NPs and Au-ZnO HNs, respectively. To inspect the repeatability of the photocatalytic activity of Au-ZnO HNs, the experiment of the photodegradation of MO with Au-ZnO HNs was repeated several times or after aged 90 days. To guarantee the veracity of the experiments, it has been used the same samples of ZnO NRs before and after combined with Au NPs for photocatalytic experiment. The stock solution of MO (8 ml, 2.5 ppm) was prepared. One set of ZnO NRs sheets (4 pieces, 12×12 mm^2), one set of Au NPs samples (4 pieces, 12×12 mm^2) and the other one of Au-ZnO HNs (4 pieces, 12×12 mm^2) were used. Figure. 6 presents the photodedegradation effects of MO with Au-ZnO HNs (red line) or ZnO NRs (blue line) or Au NPs (orange line) under UV light. As comparison, the degradation effect of MO under UV lamp is also illustrated (green line). There was seems no degradation for MO with or without ZnO NRs and Au NPs (green line, orange line and blue line). In the meantime, most interesting, an enhanced photocatalytic activity for Au-ZnO HNs could be found (red line). It could rationally attribute such enhanced photocatalytic activity of Au-ZnO HNs to the charges separation of photo-generated electrons and holes in metal-semiconductor HNs. When the electrons are excited from the V-band to the C-band of ZnO by UV light, the photo-generated holes are still in the V-band. It is well known that there would be the same Fermi level in the metal-semiconductor heterosturcture due to the built-in electric field near the interface, hence, both energy bands of metal and semiconductor will bend. Accordingly, the location of Fermi level of Au near the interface is below the C-band of ZnO.[34] So the excited electrons would flow to the Au NPs causing the separation of photo-generated electrons and holes, further leading to the suppression of their recombination, final giving rise to achieve high photocatalytic performance. Figure. 7 shows the stability of as-prepared Au-ZnO HNs which kept high photocatalytic activity after several repetitions or aged 90 days. Figure. 1d also shows the stability performance of Au-ZnO HNs after 4 h photocatalysis. Because of the charge transfer of electrons and holes, a large number of photogenerated electrons and holes were consumed in photocatalysis, a small number of the photogenerated hole would take a part in oxidation and corrosion of ZnO NRs to improve the stability of Au-ZnO HNs.

In the controlled experiments, gold had also been deposited on ZnO NRs array with magnetron sputtering for 15 or 60 seconds and annealed at 200 ^oC for 2h. It is found, however, that the corresponding photocatalysis performances (not shown) were not as good as that of 30 seconds. The length of gold sputtering time would control the thickness of gold film, hence, influencing the formation of Au-ZnO HNs. For short sputtering time, say 15 seconds, the number and size of Au NPs and, hence, the quench ability of Au-ZnO HNs were limited. On the other hand, for long sputtering time, say 60 seconds, it was found that Au film could difficultly shrink to form Au particles during annealing process. For both cases, therefore, it was difficult for them to achieve the similar photocatalytic performance presented.

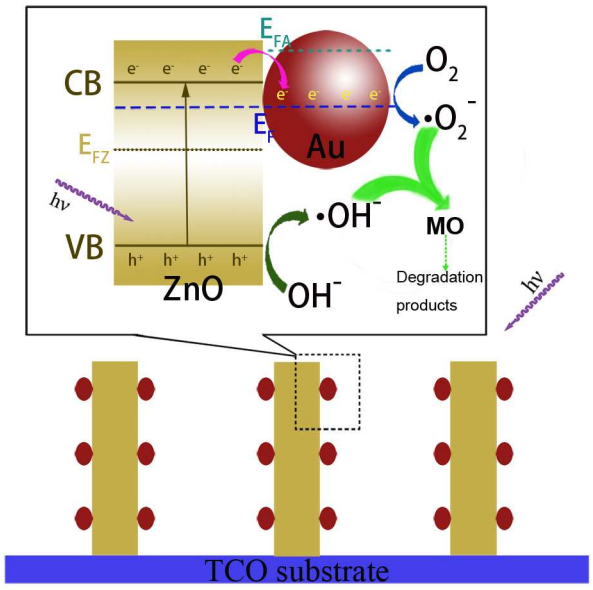

Figure. 8 Schematic diagram of mechanism of photo degradation procedure in Au-ZnO HNs.

The mechanism of charge transfer and the redox reaction in Au-ZnO HNs is shown in Figure. 8, which is, hereby, briefly discussed as below: Being a direct energy band gap material, ZnO NRs would absorb the incident photons, as the energy of which is greater than or equal to its band gap, electrons will be excited from V-band to C-band, leaving behind same amount of holes in the V-band, thus, there might be promoted a great deal of photo-induced electron-hole pairs under the proper irradiation of UV light. The Fermi level of Au is much higher than the position of C-band of ZnO. However, as the two components combine with each other to form HNs, the Fermi level of the HNs would be below the bottom of C-band of ZnO because of the equilibrium alignment of the Fermi level for metal and semiconductor heterostructure.[35] Therefore, the photoelectrons would spontaneously move from ZnO to Au.[36] Hence, Au NPs would act as a sink of photoelectrons. In the condition of without the electron collector like dye, the accumulation of photoelectrons in Au NPs leads to the separation of photo-generated electrons and holes, and indirectly suppresses the re-combination of photoinduced electrons and holes in ZnO, therefore, ultimately gives rise to the quenching of PL emission. On the other hand, because of charge transfer in Au-ZnO HNs, the recombination of photo-generated electrons and holes is suppressed and the superoxide activation process would be achieved due to the photogenerated electron-hole pairs will go on. Photogenerated electrons in Au NPs react with oxygen to produce superoxide anion radicals, $^{\bullet}O^{2-}$ while holes react with H_2O to produce hydroxyl radicals, $^{\bullet}OH^{-}$.[25, 33] Superoxide anion radicals and hydroxyl radicals will react with MO making it degrade and discolor. Similar experiments have been carried out with CdX/Me or Me-ZnO NHs (Me: Au, Ag or Pt, X: S or Se), in which 10-20 mg HNs was dispersed into the aqueous solution [25, 33, 36, 37].

Whereas, in the present study, 4 sheets of Au-ZnO HNs (12×12 mm^2) were immerged in the diluted MO aqueous solution. The weight of Au-ZnO HNs used, hereby, was about 55 μg. Thus, it is rational deduced that Au-ZnO HNs could be an efficient photo-degradation catalyst.

Conclusions

In conclusion, it has been demonstrated the preparation of Au-ZnO hybird nanostructure array on the TCO glass substrate. Meanwhile, the characterizations on the morphology and the structure of Au-ZnO hybird nanostructure reveal the prepared Au-ZnO hybird nanostructure could be of fine crystalline structure. It is rationally deduced, based on the strategy presented here, Au-ZnO hybird nanostructure can be prepared in large scaled procedure via annealing Au coated ZnO nanorods array. The Au-ZnO hybird nanostructure have also shown the much superior photocatalytic activity over ZnO nanorods in case of degradation process of MO. It is found that 8 ml methyl orange aqueous solution (2.5 ppm) could be totally degradated with 4 sheets of Au-ZnO hybird nanostructure (12×12 mm^2) within 4 hours. The preparation method discussed can also be easily expanded in nanohybrid synthesis procedure other than Au nanoparticles or ZnO nanostructures used, since Ag, Pt can play the same role as Au and ZnO can be replaced by other semi-conductor. Therefore, we can affirmatively conclude that as-prepared Au-ZnO hybird nanostructure and its manufacture method have a potential application in nanocatalysis aspect.

Notes and references

School of Materials Science and Engineering, Sichuan University
Chengdu, Sichuan, P. R. China
*Corresponding author: sunxs@scu.edu.cn

1. C. Xu, J. Xie, D. Ho, C. Wang, N. Kohler, E. G. Walsh, J. R. Morgan, Y. E. Chin and S. Sun, Angewandte Chemie International Edition, 2008, 47, 173-176.
2. H. Guo, Y. Chen, X. Chen, R. Wen, G. H. Yue and D. L. Peng, Nanotechnology, 2011, 22, 195604.
3. Y. Shemesh, J. E. Macdonald, G. Menagen and U. Banin, Angewandte Chemie International Edition, 2011, 50, 1185-1189.
4. Na Liang, Jiaotao Zai, Miao Xu, Qi Zhu, Xiao Wei and Xuefeng Qian, J Mater Chem A, 2014, 2, 4208.
5. Na Liang, Min Wang, Lun Jin, Shoushuang Huang, Wenlong Chen, Miao Xu, Qingquan He, Jiantao Zai, Nenghu Fang, and Xuefeng Qian, ACS Appl Mater Interfaces, 2014, 6, 11698.
6. A. Y. Lin, J. K. Young, A. V. Nixon and R. A. Drezek, Small, 2014, 10, 3246-3251.
7. Y. Zhou, L. Hao, S. Yu, M. You, Y. Zhu and Z. Chen, Chem Mater, 1999, 11, 3411-3413.
8. N. T. K. Thanh and L. A. W. Green, Nano Today, 2010, 5, 213-230.
9. H. Zhang, X. Fan, X. Quan, S. Chen and H. Yu, Environ Sci Technol, 2011, 45, 5731-5736.
10. E.H. Espinosa, R. Ionescu, B. Chambon, G. Bedis, E. Sotter, C. Bittencourt, A. Felten, J. Pireaux, X. Correig and E. Llobet, Sensors and Actuators B: Chemical, 2007, 127, 137-142.
11. Z. Wen, Q. Wang, Q. Zhang and J. Li, Adv Funct Mater, 2007, 17, 2772-2778.
12. J. H. Bang and P. V. Kamat, ACS Nano, 2009, 3, 1467-1476.
13. T. Torimoto, S. Ogawa, T. Adachi, T. Kameyama, K. Okazaki, T. Shibayama, A. Kudo and S. Kuwabata, Chem Commun, 2010, 46, 2082.
14. J. M. Luther, J. Gao, M. T. Lloyd, O. E. Semonin, M. C. Beard and A. J. Nozik, Adv Mater, 2010, 22, 3704-3707.
15. K. Hosono, I. Matsubara, N. Murayama, S. Woosuck and N. Izu, Chem Mater, 2005, 17, 349-354.
16. J. Gao, K. Chen, R. Xie, J. Xie, S. Lee, Z. Cheng, X. Peng and X. Chen, Small, 2010, 6, 256-261.
17. R. Costi, A. E. Saunders, E. Elmalem, A. Salant and U. Banin, Nano Lett, 2008, 8, 637-641.
18. K. Wu, H. Zhu, Z. Liu, W. Rodríguez-Córdoba and T. Lian, J Am Chem Soc, 2012, 134, 10337-10340.
19. K. Wu, Z. Chen, H. Lv, H. Zhu, C. L. Hill and T. Lian, J Am Chem Soc, 2014, 136, 7708-7716.
20. Z. L. Wang, Journal of Physics: Condensed Matter, 2004, 16, R829-R858.
21. Zhuo Wang, Xue-feng Qian, Yi Li, Jie Yin, Zi-kang Zhu, J Solid State Chem, 2005, 178, 1765.
22. Zhi Li, Xue-feng Qian, Jie Yin, Zi-kang Zhu, J Solid State Chem, 2005, 178, 1589.
23. Y. Chen, D. Zeng, K. Zhang, A. Lu, L. Wang and D. Peng, Nanoscale, 2013, 6, 874.
24. P. Li, Z. Wei, T. Wu, Q. Peng and Y. Li, J Am Chem Soc, 2011, 133, 5660-5663.
25. S. Kuriakose, V. Choudhary, B. Satpati and S. Mohapatra, Phys Chem Chem Phys, 2014, 16, 17560.
26. C. Ren, B. Yang, M. Wu, J. Xu, Z. Fu, Y. Lv, T. Guo, Y. Zhao and C. Zhu, J Hazard Mater, 2010, 182, 123-129.
27. Y. Zhang, J. Xu, P. Xu, Y. Zhu, X. Chen and W. Yu, Nanotechnology, 2010, 21, 285501.
28. J. W. Chiou, S. C. Ray, H. M. Tsai, C. W. Pao, F. Z. Chien, W. F. Pong, C. H. Tseng, J. J. Wu, M. H. Tsai, C. H. Chen, H. J. Lin, J. F. Lee and J. H. Guo, The Journal of Physical Chemistry C, 2011, 115, 2650-2655.
29. K. X. Yao, X. Liu, L. Zhao, H. C. Zeng and Y. Han, Nanoscale, 2011, 3, 4195.
30. C. Pacholski, A. Kornowski and H. Weller, Angewandte Chemie, 2004, 116, 4878-4881.
31. B. Xue, Y. Liang, L. Donglai, N. Eryong, S. Congli, F. Huanhuan, X. Jingjing, J. Yong, J. Zhifeng and S. Xiaosong, Appl Surf Sci, 2011, 257, 10317-10321.
32. K. Vanheusden, C. H. Seager, W. L. Warren, D. R. Tallant and J. A. Voigt, Appl Phys Lett, 1996, 68, 403.
33. Q. Wang, B. Geng and S. Wang, Environ Sci Technol, 2009, 43, 8968-8973.
34. V. Subramanian, E. E. Wolf and P. V. Kamat, The Journal of Physical Chemistry B, 2003, 107, 7479-7485.
35. L. Jing, W. Zhou, G. Tian and H. Fu, Chem Soc Rev, 2013, 42, 9509.
36. Y. Zheng, L. Zheng, Y. Zhan, X. Lin, Q. Zheng and K. Wei, Inorg Chem, 2007, 46, 6980-6986.
37. S. Liu and Y. Xu, Nanoscale, 2013, 5, 9330.